ION AND PROTON LOSS PATTERNS AT THE SPS AND LHC

R. Bruce, R. Assmann, G. Bellodi, C. Bracco, H.H. Braun, S. Gilardoni,
J.M. Jowett, S. Redaelli, T. Weiler, CERN, Geneva, Switzerland

Abstract

The collimation system of the LHC, primarily designed for proton operation, must function safely also with $^{208}\mathrm{Pb}^{82+}$ions. However, the particle-matter interaction in a collimator is different for heavy ions and protons. Heavy ions are subject to nuclear fragmentation, which creates a spectrum of secondary particles exiting the collimators with a Z/A ratio different from the nominal beam. These particles could be lost in a superconducting magnet and the induced heating might cause a quench. The program ICOSIM has previously been used to simulate these losses in the LHC. In this article, we present a benchmark of ICOSIM, using measured proton and ion loss maps in the SPS, and find a good qualitative agreement. We also make a quantitative comparison where the showers of the lost particles are simulated with the FLUKA code in the full magnet geometry. Here a discrepancy of a factor 3.8 is found. Estimation of expected uncertainties continues.

INTRODUCTION

The LHC requires a very efficient collimation system, since the beams have higher intensities than ever before and at the same time the superconducting magnets are very sensitive to heating and might thus quench due to lost beam particles. This is achieved with a two-stage collimation system [1, 2]: Short primary collimators intercept halo particles and give them an angular kick caused by multiple scattering, so that they, possibly several turns later, are intercepted by the longer secondary collimators where they deposit their energy through a hadronic shower. Both primary and secondary collimators are made of graphite because of its low stopping power and good heat transfer characteristics. This system has been primarily designed to meet the tight requirements for proton operation.

However, the LHC will also collide $^{208}\mathrm{Pb}^{82+}$ion beams during approximately one month per year, and necessary precautions have to be made for heavy ion operation in order to make sure that beam losses are within acceptable limits. The main parameters of the $^{208}\mathrm{Pb}^{82+}$and proton beams are summarized in Tab. 1. Although the stored energy in the $^{208}\mathrm{Pb}^{82+}$beam is only 3.81 MJ, compared to the 350 MJ in the proton beam, the ion collimation efficiency is much lower [3]. This is caused by the different particle-matter interaction in the collimator jaws. The nuclear interaction length is 2.2 cm for 2.76 TeV/nucleon $^{208}\mathrm{Pb}^{82+}$ions in graphite as opposed to 38.1 cm for 7 TeV protons, although multiple scattering angles are very similar. The nuclear interactions, together with electromagnetic dissociation, split up the nucleus into smaller fragments. This means that the ions have a high probability of fragmenting in the primary collimator before they have obtained the necessary angular deviation to be intercepted by the secondary jaws.

Table 1: LHC beam parameters for $^{208}\mathrm{Pb}^{82+}$and p$^+$ operation (nominal collision).

	$^{208}\mathrm{Pb}^{82+}$ions	Protons
Energy per nucleon	2.76 TeV	7 TeV
Number of bunches	592	2808
Particles per bunch	7×10^7	1.15×10^{11}
Bunch spacing	100 ns	25 ns
Peak luminosity	10^{27} cm^{-2} s^{-1}	10^{34} cm^{-2} s^{-1}
Stored beam energy	3.81 MJ	350 MJ

The fragmented ions leaving the primary collimator have different Z/A ratios, and thus different magnetic rigidities equivalent to a fractional momentum deviation of

$$\delta = \frac{AZ_0}{A_0 Z} - 1 \qquad (1)$$

with A_0 and Z_0 being the mass and charge numbers of the nominal beam. Therefore, these ions follow the locally generated dispersion function d_x from the primary collimator and are lost where the horizontal aperture A_x satisfies

$$A_x = \delta d_x. \qquad (2)$$

This is likely to happen outside the warm regions of the LHC, where the dispersion has grown sufficiently large. It is therefore vital to have a good quantitative understanding of these processes, in order to ensure safe operation of the LHC uninterrupted by magnet quenches.

THE ICOSIM CODE

In order to simulate the particle propagation through the LHC lattice, linked with particle-matter interactions in the collimators, a specialized code, ICOSIM [3], has been developed. ICOSIM creates an initial beam distribution that is tracked through a lattice read in from optics files and aperture tables created by MAD-X [4]. Particles are tracked using a linear matrix formalism but chromatic effects at leading order and sextupoles in thin kick approximation are also included. Beam acceleration is not taken into account, since the RF synchrotron oscillation period is about 500 turns at collision.

ICOSIM has a simple built-in Monte-Carlo code for simulating the interactions in the collimator, including

multiple scattering (described by a Gaussian approximation, see Chap. 23 in Ref. [5]), ionization through the Bethe-Bloch formula, nuclear fragmentation and electromagnetic dissociation. The last two processes are simulated through tabulated cross sections calculated with the abrasion-ablation [6] and RELDIS [7] models.

We have also implemented the possibility of treating the collimator interactions in an external Monte-Carlo code, which performs the transport through the collimator geometry and gives residual particles back to the tracking. Both FLUKA [8, 9] and MARS [10] have been used with similar results. These codes include more complete physics but slow down the tracking considerably. Linking with an external Monte-Carlo program is necessary when simulating proton interactions, since the built-in physics models of ICOSIM only handle ions.

RESULTS FOR THE LHC

The simulated LHC ion loss maps from ICOSIM have been presented elsewhere [3, 11, 12]. Here we will give a short summary.

An example of the loss pattern at top energy found downstream of IR7 (betatron cleaning region) is shown in Fig. 1. This simulation was done using standard settings (primary collimators at 6 σ, secondary at 7 σ and tertiary at 10 σ). Also the TCLA absorbers were included.

ICOSIM first calculates only relative magnitudes of the losses at different positions in the machine. To find the expected heating power this loss map is normalized by the beam intensity (as given in Tab. 1) and the beam life time, which is of course not well known. As a worst-case estimate the minimum allowed life time of 12 minutes was used.

It is clear that the expected heating power from beam losses well exceeds 8.5 W/m, which is an estimate of the average quench limit according to Ref. [13]. However, the quench limit depends also on factors such as magnet type and distribution of the beam losses within a given magnet and is thus not well known. There are ongoing studies on this in the AT department at CERN.

At top energy, a collimation inefficiency of 4-5% was found (defined as ratio of the number of particles lost on the aperture over the number stopped in the collimators at a particular turn of the machine), which is several orders of magnitude higher than the required value for the proton beam [14]. Similar results were found for beam 1 and 2. At injection energy the heating power is lower by a factor 20-50 which, together with the fact that the quench limit is higher, should mean that these beam losses are within acceptable limits.

Apart from the already mentioned uncertainty in the quench limit, and the uncertainty in the assumed beam lifetime, there are other factors which might introduce errors in the final result. The nuclear cross sections for ion-matter interaction in the collimators might have up to 50% error margins, and there is also an uncertainty in the impact dis-
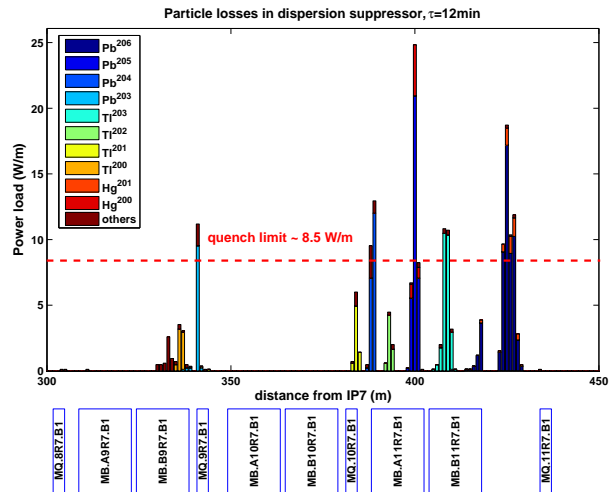

Figure 1: (color online) The loss map form ICOSIM for the dispersion suppressor after IP7 in the LHC. The estimated quench level from Ref. [13] is indicated.

tribution of the beam particles on the collimators, since the beam dynamics of the halo is not well known.

Because of these uncertainties in the ICOSIM result, a benchmark of the code is needed; we describe this in the following sections.

PROTON BENCHMARK IN THE SPS

At CERN, the two possible ways of testing the ICOSIM results are with proton or $^{208}Pb^{82+}$ ion beams in the SPS, using a prototype secondary LHC collimator, which has been installed in LSS5 [15]. The aperture and the lattice within the vicinity of the installation are shown in Fig. 2. The collimator consists of two graphite jaws, which can be moved independently to collimate the beam in the horizontal plane. This was done during circulating beam operation, and the induced beam losses were recorded by the 216 beam loss monitors (BLMs) placed around the ring.

In this section we describe the results of the measurements with proton beams, and in the next section we describe corresponding measurements with ions. Data were collected during proton operation in dedicated MD sessions in 2006 and 2007 with 270 GeV coasting beam. Typical collimator steps ranged from a few hundred micrometers up to a mm, although some larger steps up to a cm were performed.

A typical example of a recorded loss map from September 2007 is shown in Fig. 3, together with the corresponding simulated loss map from ICOSIM linked with MARS. The detector background, consisting of noise and other beam losses that are not caused by the collimator movement, had to be subtracted. As background we used the loss map from the machine cycle before the collimator movement. A similar approach was already used in Ref. [15] to benchmark simulation results from the SixTrack code.
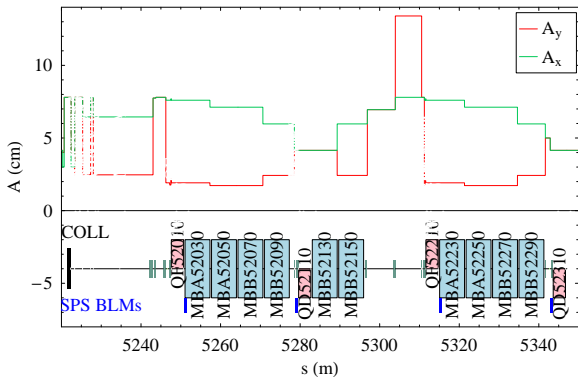
Figure 2: (color online) The aperture and beamline of the SPS just downstream of the LHC prototype collimator. Also the locations of the BLMs are indicated.
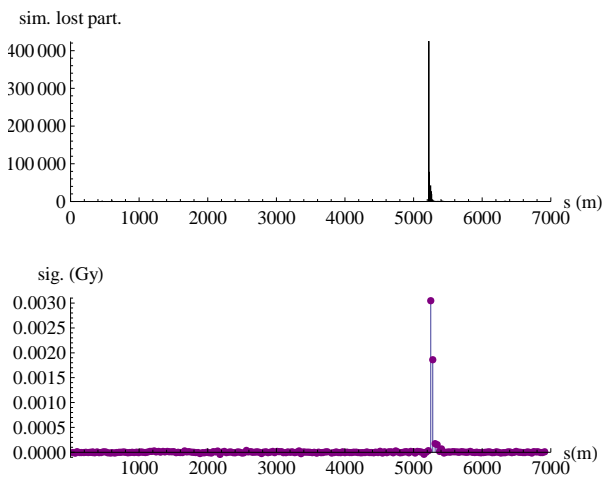

Figure 3: Simulated ICOSIM (top) and measured (bottom) proton loss map for the whole SPS ring. The collimator is located at $s = 5222$ m, just before the large loss peak.

As might be expected, the main loss location is just downstream of the collimator, which is very well reproduced by the simulation. In order to make a quantitative comparison with data, we need to consider the actual magnitude of the BLM signals. This can not be directly inferred from the ICOSIM loss maps, although we can make a rough estimate by simply counting the number of protons lost close to each BLM. In Fig. 4 the normalized average measured signal of the four closest BLMs after the collimator is shown, together with the number of particles impacting within a 2 m interval before each chamber. As can be seen, the simulated ratio between the two highest locations agrees very well with measurements.

It was found in the measurements that the ratio between these four signals was almost independent of the collimator movement—when a larger fraction of the beam is scraped away, the losses increase correspondingly, keeping this ratio. This is shown for the BLM with the highest signal

(BL520 at $s = 5250$ m) in Fig. 5. Here we show the BLM signal as a function of the decay in beam current for several different collimator movements. It can be seen from the figure that this is an approximately linear function, except when the BLM begins to saturate. This motivates why we can use the average ratio in Fig. 4.

In a general case this linear assumption might be false— a simple example of this is changing the angles of the collimator jaws and thereby the effective length travelled by the particles inside the collimator. This changes the ratio of particles lost in the collimator and the ring. In the measurements considered here however, the jaws were approximately centered around the beam. The linear behaviour is also confirmed by ICOSIM simulations, which show that the relative loss pattern stays approximately constant regardless of the distance to which the jaws are moved in.
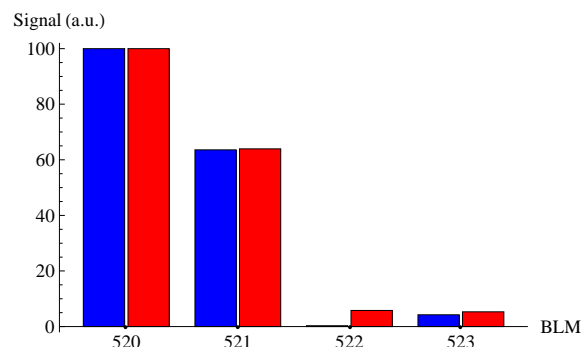

Figure 4: (color online) Average measured loss map with background subtracted over several cycles (light gray, red online) and simulated number of protons lost within a 2 m interval before each BLM (dark gray, blue online) normalized to the highest peak for the four BLMs closest to the collimator downstream.
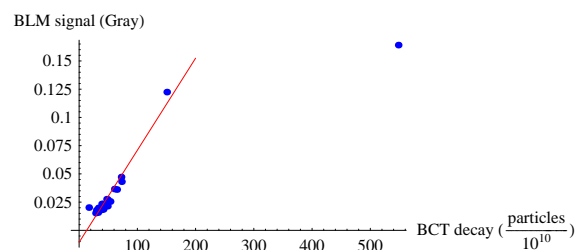

Figure 5: The highest BLM signal, from monitor BL520, as a function of the measured decay in beam current during several different collimator movements. Except for the last point to the right, where the BLM is likely to be saturated, the behaviour is approximately linear. A straight line has been plotted to guide the eye.

The smaller loss peaks in other parts of the ring were fluctuating in a seemingly random pattern between different measurements. This could be for instance due to orbit variations. In some of the measured loss maps, the second largest peak was found at $s \approx 600$ m, corresponding to the

second largest peak also in the simulation. An example of a measured and a simulated loss map for this part of the machine is shown in Fig. 6. There is also a simulated loss at $s \approx 460$ m, which could not be measured. However, the next BLM after this loss location is 15 m downstream, meaning that it might not detect these losses.
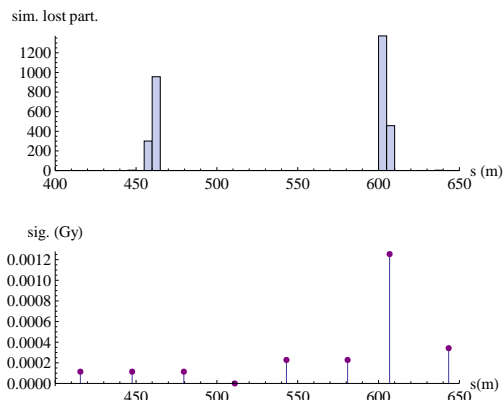

Figure 6: Simulated ICOSIM (top) and measured (bottom) proton loss map for the first part of the SPS ring.

Furthermore, smaller loss peaks were sometimes detected at $s \approx 5920$ m and 1660 m, which were not reproduced by simulations, and at $s \approx 5410$ m, which was well reproduced. A small loss peak was predicted but not measured at $s \approx 6340$ m. However, in the earlier measurements in Ref. [15], losses were detected also in this area. Generally, the loss map from ICOSIM shows a qualitatively similar behaviour to the SixTrack simulations presented in Ref. [15].

The BLM signals depend not only on the number of particles lost nearby, but also on the impact distribution of the lost particles and the amount and type of material they have to traverse before reaching the monitor. At some BLMs, with less nearby material, particles lost far away may cause a signal, while BLMs that are well shielded by magnetic elements may only see small traces of the showers caused by the closest losses. In order to accurately simulate this, the particle-matter interaction of the lost particles need to be taken into account. Thus the 3D geometry of the magnetic elements around the monitor BL520 (closest to the collimator, 30 m downstream of it) was implemented in FLUKA, as illustrated in Fig. 7. The magnetic field in the quadrupole magnet was neglected. The momenta and impact coordinates on the inside of the vacuum pipe of all particles within 10 m distance of the collimator were recorded in ICOSIM and fed as starting conditions into FLUKA and the resulting energy deposition in the N_2 gas was recorded and converted to dose in Gy. It was found from the simulations that the signal on the monitor BL520 is 0.15 mGy per 10^{10} lost particles. Comparing with measurements, the average ratio between signal and BCT current decay was found to be 0.57 mGy per 10^{10} lost particles, which is a factor 3.8 higher than simulations. This error could be due

to several factors. Apart from the systematic uncertainty in the shower simulation, and the uncertainty in the distribution of the impacting lost particles, the measurements themselves showed variations between different MDs. A detailed error estimate is ongoing work.
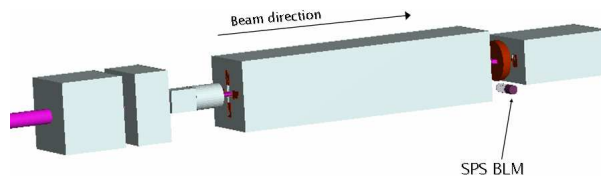

Figure 7: (color online) The geometry as implemented in FLUKA around the monitor BL520, which is located around 30 m downstream of the collimator in the SPS.

ION BENCHMARK IN THE SPS

Measurements similar to the ones described above were also carried out using coasting $^{208}\mathrm{Pb}^{82+}$ ion beams at 106.4 GeV/nucleon in the SPS in late 2007. The beam was again scraped by the collimator to induce losses in typical steps between 200 μm up to a mm. From ICOSIM loss maps, it was found that the protons are lost mainly due to angular deviations induced by the collimator, while the ions are lost due to the change in magnetic rigidity, δ, caused by fragmentation. Ions that have changed their magnetic rigidity are deterministically lost where the locally generated dispersion from the collimator and the aperture satisfy Eq. 2. This is shown in Fig. 8, where several dispersive horizontal orbits starting at the collimator are shown, for typical values of δ. It is clear from the figure that all fragments within the range $-0.09 < \delta < -0.14$ are lost at the same aperture limitation ($s = 5277$ m).

This corresponds to a large fraction of the lost fragments, and since the monitor BL521 is located only 2 m downstream of this position with almost no shielding material in between, this monitor is expected to show a high signal when ion beams are scraped with the collimator. The simulated and measured loss maps show that this is indeed the case. As can be seen in Fig. 9, showing the loss pattern for the whole ring, and Fig. 10, showing the four BLMs closest downstream of the collimator, BL521 has a signal much higher than BL520, which is closest to the collimator and where the maximum was found for protons. This is a significant qualitative difference between ion and proton operation, which is found both in simulations and measurements.

In order to verify the loss pattern quantitatively, FLUKA simulations of the particle showers should be done also for ions. We intend to do this in the future.

CONCLUSION AND OUTLOOK

We have presented preliminary results of simulated and measured beam losses in the SPS for protons and
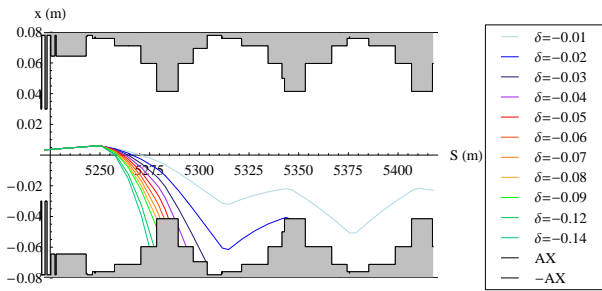
Figure 8: (color online) Dispersive orbits of fragmented ions coming out of one of the collimator jaws, shown together with the aperture. A large fraction of the total losses occur at the aperture limitation at $s = 5277$ m.
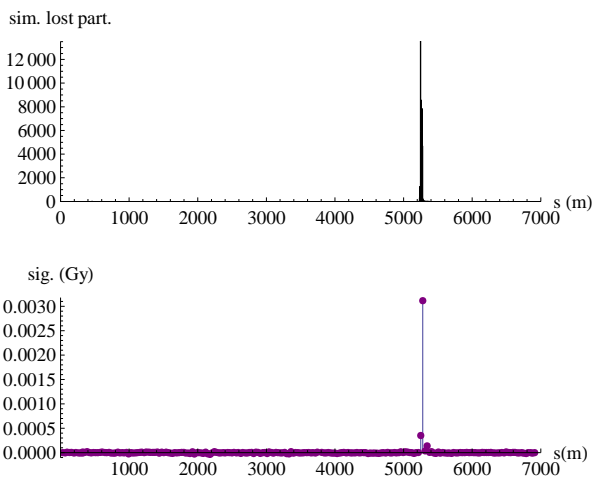

Figure 9: Simulated ICOSIM (top) and measured (bottom) ^{208}Pb^{82+} loss map for the whole SPS ring.

^{208}Pb^{82+} ions caused by movements of the collimator. In terms of comparing the ratio between different loss locations, the simulated loss patterns from ICOSIM agree well with the measured ones. However, the FLUKA simulation of the signal from proton losses in the detector with the highest signal deviated by a factor 3.8 from the measured signal. A detailed error analysis is ongoing.

We found a significant difference between the loss patterns for ^{208}Pb^{82+} ions and protons, with the maximum signal occurring at different locations, which is well understood and reproduced by ICOSIM. This is a valuable benchmark of the ICOSIM simulations carried out for the LHC.

In order to better quantify the comparison, further FLUKA simulations of the expected BLM signal for ions should be carried out. Also other monitors than BL520 should be simulated for both particle species to make a more complete analysis. This work is planned for the future.
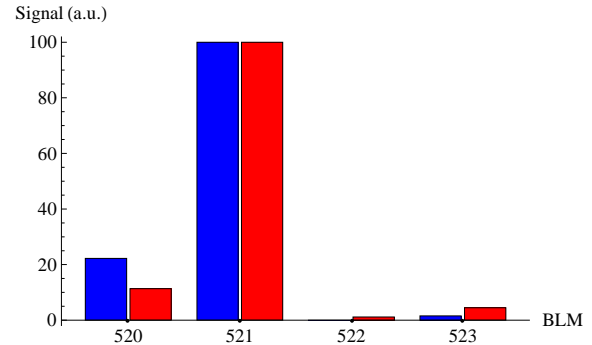

Figure 10: (color online) Average measured loss map with background subtracted over several cycles (light gray, red online) and simulated number of nucleons (number of ions$\times A_{\mathrm{ion}}$) lost within a 2 m interval before each BLM (dark gray, blue online) normalized to the highest peak for the four BLMs closest to the collimator downstream.

ACKNOWLEDGEMENTS

REFERENCES

[1] J. B. Jeanneret. Optics of a two-stage collimation system. *Phys. Rev. ST Accel. Beams*, 1(8):081001, 1998.

[2] R. Assmann et al. An improved collimation system for the LHC. *Proc. of the European Particle Accelerator Conf. 2004, Lucerne, Switzerland*, page 536, 2004.

[3] H.H. Braun. Collimation of Heavy Ion Beams in the LHC. *Proc. of the European Particle Accelerator Conf. 2004, Lucerne, Switzerland*, page 551, 2004.

[4] http://cern.ch/mad/.

[5] S. Eidelman *et al*. Review of Particle Physics. *Physics Letters B*, 592:1+, 2004.

[6] J.-J. Gaimard and K.H. Schmidt. Review of Particle Physics. *Nucl. Phys. A*, 531:709, 1991.

[7] I.A. Pshenichnov *et al*. Mutual heavy ion dissociation in peripheral collisions at ultrarelativistic energies. *Phys. Rev. C*, 64:024903, 2001.

[8] A. Fasso *et al*. FLUKA: a multi-particle transport code. *CERN Report CERN-2005-10*, 2005.

[9] A. Fasso *et al*. The physics models of FLUKA: status and recent developments. *Proc. of the Computing in High Energy and Nuclear Physics 2003 Conf., La Jolla*, 2003.

[10] http://www-ap.fnal.gov/MARS/.

[11] R. Bruce et al. Monitoring Heavy-Ion Beam Losses in the LHC. *Proc. of the European Particle Accelerator Conf. 2006, Edinburgh, Scotland*, page 544, 2006.

[12] G. Bellodi et al. Beam loss monitors for heavy ion operation. *LHC Project Note 402, CERN*, 2007.

[13] J.B. Jeanneret et al. Quench levels and transient beam losses in LHC magnets. *LHC Project Report 44*, 1996.

[14] R. Assmann et al. Expected performance and beam-based optimization of the LHC collimation system. *Proc. of the European Particle Accelerator Conf. 2004, Lucerne, Switzerland*, page 1825, 2004.

[15] S. Redaelli et al. Comparison between measured and simulated beam loss patterns in thc CERN SPS. *Proc. of the European Particle Accelerator Conf. 2006, Edinburgh, Scotland*, page 1810, 2006.